This is to certify that the
thesis entitled

FUNCTIONAL AND PHARMACOLOGICAL CHARACTERIZATION OF SIXTY-FOUR PARA SODIUM CHANNEL VARIANTS FROM *DROSOPHILA MELANOGASTER* IN *XENOPUS* OOCYTES

presented by

Rachel Lee O'Donnell Olson

has been accepted towards fulfillment
of the requirements for the

M.S. degree in Entomology

Major Professor's Signature

June 12, 2006

Date

FUNCTIONAL AND PHARMACOLOGICAL CHARACTERIZATION OF SIXTY-FOUR PARA SODIUM CHANNEL VARIANTS FROM *DROSOPHILA MELANOGASTER* IN *XENOPUS* OOCYTES

By

Rachel Lee O'Donnell Olson

A THESIS

Submitted to
Michigan State University
in partial fulfillment of the requirements
for the degree of

MASTER OF SCIENCE

Department of Entomology

2006

ABSTRACT

FUNCTIONAL AND PHARMACOLOGICAL CHARACTERIZATION OF SIXTY-FOUR PARA SODIUM CHANNEL VARIANTS IN *XENOPUS* OOCYTES

By

Rachel Lee O'Donnell Olson

Extensive alternative splicing and RNA editing of *para,* the voltage-gated sodium channel of *Drosophila melanogaster,* has been documented. However, the functional consequences of these post-transcriptional modifications have not yet been investigated. In this study we report the isolation, expression, and functional characterization of sixty-four full-length *para* cDNA clones. The sixty-four clones were grouped into twenty-nine splice types based on alternative exon usage. Functional analysis of these variants revealed a broad spectrum of voltage-dependences of activation and to a lesser extent, voltage dependences of inactivation. Sequence comparison of three functionally distinct variants uncovered novel A to I editing sites. Furthermore, differential sensitivities to an α-scorpion toxin, LqhαIT, were revealed. The observed functional and pharmacological diversity of para variants supports the notion that alternative splicing and RNA editing are the two major mechanisms for generating sodium channel diversity in insects.

ACKNOWLEDGMENTS

I would like to express my sincere thanks to Dr. Ke Dong for providing me with this opportunity, her guidance, support, and encouragement throughout the course of my master's research.

I would also like to thank Dr. Robert Hollingworth, Dr. Suzanne Thiem, and Dr. Edward Walker for their guidance and support.

Appreciation is also extended to the members of Dr. Ke Dong's laboratory. I would like to thank Dr. Weizhong Song and Dr. Yuhze Du for teaching me electrophysiological techniques, Mrs. Yoshiko Nomura for her assistance and instruction in molecular biology techniques, and Dr. Zhiqi Liu for cloning sixty-four *para* variants providing the foundation for my thesis work. A special thanks is also extended to Dr. Kristopher Silver for his critical review of my thesis.

I would finally like to express my appreciation for the support and encouragement I received during the course of this research from my husband Rory Olson, and my parents Ruth and Jim O'Donnell.

TABLE OF CONTENTS

LIST OF TABLES AND FIGURES FOR CHAPTER 1

LIST OF TABLES AND FIGURES FOR CHAPTER 3

CHAPTER 1: Literature Review

I. Discovery of Sodium Current

Action potentials are electrical signals by which excitable cells, such as neurons, receive, conduct, and transmit information. In a series of elegant experiments, Alan Hodgkin and Andrew Huxley demonstrated that action potentials are the result of ions moving through the plasma membrane (Hodgkin and Huxley, 1952 a, b). Furthermore, they established sodium as one of the ions responsible for the production of action potentials and hypothesized that sodium selective pores activate (open) and inactivate (close) in response to changes in membrane potential. Because of their significant discovery the Nobel Prize was appropriately awarded to Alan Hodgkin and Andrew Huxley.

II. Isolation of the Sodium Channel Protein

The proteins that comprise the voltage-gated sodium channel (SC) have been purified from a variety of tissues and species (review by Catterall, 2000). Using the high affinity binding of the SC protein to a radioactive-labeled tetrodotoxin, the protein was first purified from the electric organ of the eel, *Electrophorus electricus* (Agnew et al. 1980). This purified SC consists of a single polypeptide of an approximate weight of 270 kDa. Subsequent photo-affinity labeling experiments using a sodium specific neurotoxin, α-scorpion toxin, led to the discovery of two peptides (36 and 260 kDa) from synaptosomal membranes of the rat brain. The isolated peptides are denoted as α (primary) and β (auxiliary) subunits of the SC. The α polypeptide corresponds to the 270 kDa polypeptide isolated from eel (Beneski and Catterall, 1980).

III. Molecular Biology of the Sodium Channel

With the development of molecular biology techniques, our understanding of the molecular biology of voltage-gated sodium channels has greatly advanced. The major achievements and discoveries are summarized below.

III. A Cloning of the First α-Subunit cDNAs

Sodium channel α-subunit cDNAs were isolated from electric eel by screening expression libraries of electroplax eel mRNA using oligonucleotides encoding the electric eel SC and antibodies against the eel SC protein (Noda et al., 1984). Sequencing the entire polypeptide from the deduced cDNAs revealed the primary amino acid structure of the SC. The secondary structure of the α-subunit was determined to have four homologous domains (DI – DIV), each consisting of six transmembrane segments (S1 – S6) (Noda et al., 1984; review by Catterall, 2000).

III. B Functional Expression of the α-Subunit

Expression of the pore-forming α-subunit alone generates sodium currents in *Xenopus* oocytes and mammalian cell lines (Noda et al., 1986). However, channel gating and expression are modulated by the inclusion of β subunits and result in emulating channels *in vivo* (reviewed by Catterall, 2000). A total of four β subunits have been identified in mammals (β1, β2, β3, & β4) (Yu et al., 2003). These subunits are hypothesized to function as cell adhesion molecules involved in cell-to-cell interactions. It is important to note that the expression of α and β subunits varies between tissues (reviewed by Isom, 2001). For example, the

skeletal muscle sodium channel is a complex of α and $\beta 1$ subunits, whereas, the mammalian brain is comprised of α, $\beta 1$, and $\beta 2$ subunits.

III. C The Molecular Basis of Sodium Channel Function

Molecular mechanisms pertaining to the structure-function relationship of mammalian SCs have been and are currently under investigation. Below is our current understanding of the molecular basis of SC function.

III. C1 Outer and Inner Pores, Selectivity Filter

The outer pore (extracellular opening) and selectivity filter (amino acids that confer the channel to be sodium selective) of the channel is formed by the membrane re-entrant loops connecting segments 5 and 6 of domains I-IV (Catterall, 2000). The neurotoxins tetrodotoxin (TTX) and saxitoxin (STX) block the SC by binding to the outer pore and thereby preventing sodium ion entry into the cell (Hille, 1984). A pair of amino acids located in each reentrant loop was associated with TTX and STX binding along with forming the selectivity filter (Hille, 1984; Terlau et al., 1991). The outer most set of amino acids, EEDD, form the outermost ring of the channel and serve as the primary binding site of these neurotoxins, which led to the identification of the outer pore (Fig. 1). The amino acid residues DEKA form the selectivity filter in the innermost part of the outer pore (Fig. 1; Terlau et al., 1991). Mutating DEKA to EEEE causes the SC to become permeable to calcium ions (Heinemann et al., 1992). The inner pore (intracellular portion) of the SC is proposed to be formed by the S6 segments (Fig. 1; Striessnig et al., 1990), which is based on evidence that local anesthetics (LAs) enter and bind to residues in the S6 segments and block the pore from the intracellular side (Hille, 1984).

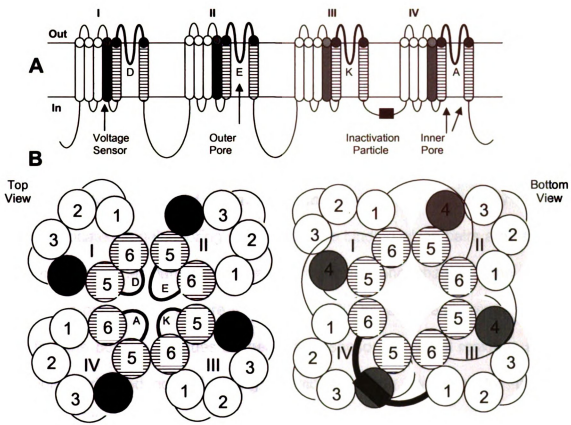

Figure 1 A-B Topological transmembrane organization of the voltage-gated sodium channel. **A.** The α-subunit of the SC consists of four homologous domains (DI-DIV) each containing six transmembrane segments (S1-S6). Voltage-sensors are formed by the S4 segments in each domain (grey). The outer pore and selectivity filter are formed by the linker connecting S5-S6 of all four domains (striped). The sodium-selective-filter is formed by the amino acids DEKA. The inactivation particle containing the IFMT motif is located on the D3-D4 loop. The inner pore is formed by the arrangement of the segments 5 and 6. **B.** Schematic transmembrane arrangement of DI-DIV of the α-subunit forming the channel pore. The linker connecting S5-S6 of each domain form the outer pore and contain the amino acids DEKA (top view). The S6 segments form the inner pore and are depicted by the bottom portion of the S6 cylinders being tilted inwards.

III. C2 S4 Segments; Activation

A depolarization of the membrane electric field leads to activation of the sodium channel (Hodgkin and Huxley 1952a). Each S4 segment contains four to eight positively charged arginine or lysine residues separated from each other by

two neutral residues. These positively charged S4 segments serve as a voltage sensor and respond to potential changes across the plasma membrane (Fig. 1; Noda et al. 1984). Two comparable models have been proposed to explain the mechanism underlying activation; the sliding helix and the helical screw (Catterall, 1986; Guy and Seetharamulu, 1986). Both models assume that the positive residues of the S4 segments form ion pairs with negatively charged residues located in neighboring segments. The binding of ion pairs are released upon membrane depolarization, causing a conformational change of the channel resulting in opening of the pore (Catterall, 1986; Guy and Seetharamulu, 1986). Mutating the positive residues of the voltage sensor to neutral residues altered the voltage-dependency of gating, providing strong evidence for the two proposed activation models (Stuhmer et al., 1989; Kontis et al., 1997). The outward movement of the S4 segments in response to depolarization was detected in an elegant set of cysteine scanning mutagenesis experiments, further establishing the role of S4 as voltage sensors in sodium channels (Refs. in Catterall, 2000).

III. C3 The IFMT Motif; Inactivation.

Inactivation of the sodium channel occurs within a few milliseconds after activation, closing the channel pore (Ulbricht, 2005). Site-directed antibody and site-directed mutagenesis studies revealed that the short intracellular linker connecting DIII to DIV plays an integral role in fast inactivation (Fig. 1) (Refs. in Catterall, 2000). A contiguous hydrophobic triad of isoleucine, phenylalanine, and methionine (IFM) positioned in the middle of this linker are crucial for fast inactivation (West et al., 1992). Site-directed anti-peptide antibodies to this linker

(Vassilev et al., 1988, 1989), deletions of amino acids from this loop (Patton et al., 1992), as well as mutating the IFM triad to glutamate (QQQ) inhibited inactivation (West et al., 1992). Additional experiments demonstrated that peptides containing the IFM motif serve as pore blockers to inactivation deficient channels and completely restore inactivation, providing further evidence supporting the significant role of the IFM motif in inactivation (Eaholtz et al., 1994; McPhee 1998; Eaholtz et al., 1999). Recent experiments indicate that there is a fourth amino acid, threonine, in addition to the IFM triad, that is essential for fast inactivation (IFMT) (Rohl et al., 1999).

Inactivation occurs with the occlusion of the pore resulting in the block of further ion entry into the cell (review by Goldin, 2003). The small linker connecting DIII to DIV (containing the IFMT motif) is responsible for occlusion of the pore by binding to hydrophobic residues near the intracellular portion of the channel. Scanning mutagenesis experiments indicate that the docking site of the IFMT motif consists of the S4-S5 linkers of DIII and DIV along with the cytoplasmic portion of DIVS6. It is hypothesized that the conformational change ensued by the S4 segments result in the exposure of the hydrophobic residues contained in the S4-S5 segments which then interact with the IFMT motif, locking it into place.

Binding of the IFMT motif to its docking site is thought to be facilitated by glycine and proline residues that flank the short intracellular linker connecting DIII to DIV. Glycine residues confer flexibility in protein structure as proline residues offer structural rigidity and a bent conformation to the linker (refs. in Zhao et al., 2004). The flexibility of glycine and the structural rigidity of proline serve as

'molecular hinges' for the small linker containing the IFMT motif. Thus, the linker connecting DIII to DIV has been described as a 'hinged lid' with the IFMT motif acting as a 'latch', locking the lid into place by binding to the intracellular portion of the pore and preventing further ion entry into the cell (described as a 'hinged lid' model; review by Catterall, 2000).

IV. Mammalian Voltage-Gated Sodium Channels

Voltage-gated sodium channel genes have been identified in various vertebrates and invertebrates such as humans, rats, leaches, fish, and several species of insects (review by Goldin, 2002). Nine different SC α-subunit genes, $Na_V1.1$ – $Na_V1.9$, have been identified in mammalian systems (Goldin et al. 2000; Catterall et al. 2003). These nine mammalian SC proteins share greater than 50% amino acid homology (Goldin et al. 2000). These SCs are expressed in different tissues and cell types and are localized in different sub-cellular compartments. Each has unique gating properties thought to fulfill distinctive roles in a given cell type. Mutations in the SC genes have been associated with various mammalian diseases including myoclonic epilepsy of infancy and hyperkalemic periodic paralysis (Claes et al., 2001; Kelly et al., 1997).

IV.A Tissue-Specific Expression

The nine isoforms of the mammalian SC exhibit distinct tissue distribution patterns. Transcripts of most isoforms are present in many different tissues, however, the abundance of each isoform is profound in only select tissues (review by Goldin, 1999). Isoform $Na_V1.1$ is abundantly expressed in the central nervous system (CNS) along with $Na_V1.2$ and Na_V 1.3. Additionally, $Na_V1.1$ and $Na_V1.3$ are localized to the somas of neurons, while $Na_V1.2$ was detected in the

nodes of Ranvier and in unmyelinated axons. $Na_V1.4$ is specifically expressed in skeletal muscle and $Na_V1.5$ is independently expressed in cardiac myocytes. Isoform $Na_V1.6$ is most abundant in the CNS in comparison to the peripheral nervous system (PNS) but is also detected in dorsal root ganglia (DRG) neurons. $Na_V1.7$ is mainly expressed in the PNS, being present in DRG neurons, Schwann cells, and in neuron-endocrine cells. The last two isoforms, $Na_V1.8$ and $Na_V1.9$, have been identified in the PNS DRG neurons and trigeminal ganglia.

IV.B Developmental-Specific Expression

Besides tissue-specific expression patterns, developmental specific-regulation of mammalian SCs have been documented for seven of the nine isoforms ($Na_V1.1$ - $Na_V1.7$; review by Goldin, 1999). $Na_V1.1$ becomes detectible shortly after birth and increases in number until adulthood. Na_V 1.2 is accumulated in embryonic nodes of Ranvier in some CNS tracts. The transcription level of isoform $Na_V1.3$ peaks at birth and becomes undetectable in adulthood. Transcripts of Na_V 1.5 are detectable in neonatal skeletal muscle but are replaced by Na_V 1.4 in adult skeletal muscle. Na_V 1.6 is the most abundantly expressed isoform found in the CNS during adulthood, but, is expressed in lower numbers during development. Transcripts of Na_V 1.7 are located in the neonatal cortex of the CNS The remaining two isoforms, Na_V 1.8 and Na_V 1.9, have not yet been described to display developmental-specific expression patterns (review by Goldin, 1999).

IV.C Unique Electrophysiological Gating Properties of Mammalian SCs

The nine SC variants in mammals exhibit significant differences in functional properties. These differences likely contribute unique functional roles

in distinct tissues or cell types. Specifically, the voltage required for activation and inactivation varies among the isoforms (Table 2).

Table 1. Tissue-specific and developmental-specific expression patterns of the nine mammalian voltage-gated sodium channels

SC Type	Primary Tissue Distribution	Developemental Profile
$Na_V1.1$	CNS	adult
$Na_V 1.2$	CNS	adult
$Na_V 1.3$	CNS	fetus
$Na_V 1.4$	skeletal muscle	adult
$Na_V 1.5$	heart muscle	adult
$Na_V 1.6$	CNS	adult
$Na_V 1.7$	PNS	neonatal
$Na_V 1.8$	PNS	
$Na_V 1.9$	PNS	

Table modified from Goldin, 1999

V. Insect Voltage-Gated Sodium Channel

It is important to study insect SCs for three key reasons. First, SCs are targeted sites of several classes of insecticides, including DDT, pyrethroids, and indoxacarb (Soderlund, 2005). These insecticides are widely used in the control of agricultural and medically related pest species. However, resistance to current insecticides is a global problem. Mutations in the SC gene have already been shown to confer resistance to pyrethroids and DDT (Soderlund, 2005). Second, as presented below, the insect SC gene undergoes extensive post-transcriptional modifications including alternative splicing and RNA editing events. At the present time, we do not understand the contributions of alternative splicing and RNA editing in the regulation of neuronal excitability. Third, though there is great

similarity in the structure-function relationships between the insect and mammalian channels, pharmacological differences have been reported (Cestele and Catterall, 2000). Thus, by better understanding the molecular basis of differential sensitivities of insect and mammalian SCs to various neurotoxins, valuable information will be provided toward the development of safe and selective insecticides.

Table 2. Gating properties of nine mammalian SCs

Isoform	Activation (mV)	Inactivation (mV)	Notes
Na_V 1.1	-33	-72	
Na_V 1.2	-24	-53	
Na_V 1.3	-23 to -26	-65 to -69	
Na_V 1.4	-26	-50.1 or -56	
	-30		rat
Na_V 1.5	-47 or -56	-84 or -100	F as the major anion in intracellular solution
	-27	-61	aspartate as the major anion in intracellular solution
Na_V 1.6	-8.8	-55	cut-open oocyte clamp; mouse
	-17	-51	" " + β1& β2
	-26		" " + inactivation removed
	-37.7	-97.6	macropatch clamp; rat
Na_V 1.7	-31		macropatch; rat
	-45	-65	TTX sensitive DRG neurons
		-78	two-electrode clamp; rat
		-60.5	whole-cell clamp
		-39.6V	whole-cell clamp (+β1)
Na_V 1.8	-16 to -21	~-30	DRG neurons; rat
Na_V 1.9	-47 to -54	-44 to -54	DRG neurons; rat

Modified from Catterall, Goldin, and Waxman (2005).

V.A Isolation of the *Drosophila* Voltage-Gated Sodium Channel Gene

In 1987 the *Drosophila* sodium channel 1 (DSC1) was isolated by screening a *Drosophila* genomic library with a cDNA probe encoding the eel SC.

The deduced amino acid sequence of DSC1 revealed high homology to that of the previously characterized vertebrate SCs. The secondary structure of DSC1 was deduced to contain four homologous domains, each containing six transmembrane segments like that of mammalian SCs. Importantly, the S4 segments of each domain of the DSC1 channel also contained positive residues separated by two uncharged resides resembling the 'voltage sensors' described in mammalian sodium channels (Salkoff et al., 1987).

In the same year, 1987, Ganetzky and colleagues isolated a second SC gene, *para*, by analyzing a temperature-sensitive paralytic phenotype of *Drosophila* mutants. These paralytic temperature-sensitive mutant flies undergo instantaneous paralysis when temperatures are elevated to 29°C but fully recover when restored to ambient temperature (22°C) (Suzuki et al. 1971; Siddiqi and Benzer, 1976). The observed paralysis was hypothesized to be the result of a temperature sensitive blockade of action potential conduction (Siddiqi and Benzer, 1976; Wu and Ganetzky, 1980). This *para* gene was isolated using P-element transposon tagging (Loughney et al., 1989). The complete Para protein was deduced from six overlapping cDNA clones and revealed four homologous domains like that described of other SCs as well as being highly homologous in the transmembrane regions (60%) to those of the rat brain channel (Loughney et al., 1989). In an independent study, the *D. melanogaster* genomic library was searched for sequences similar to rat brain SCs. This study resulted in the isolation of partial cDNAs corresponding to *para* and DSC1, suggesting that there are two genes encoding SCs in insects (Ramaswami and Tanouye, 1989).

In situ hybridization and immunochemistry studies revealed distinct tissue and developmental distribution patterns of *para* and DSC1. Using *para* and DSC1 cDNA restriction fragments as probes, the expression patterns of para and DSC1 transcripts were analyzed in *in-situ* hybridization experiments. The results of this study indicate that *para* is ubiquitously expressed throughout the nervous system in all developmental stages, while DSC1 is detected in all stages except that of the embryonic stage (Hong and Ganetzky, 1994). Additionally, *para* is expressed throughout the CNS and PNS while DSC1 is restricted to a few cells in either system (Hong and Ganetzky, 1994; Castella et al., 2001).

When functionally expressed the *para* transcripts were found to carry the inward voltage-dependent sodium current (Germeraad et al., 1992). Functional analysis of Para in *Xenopus* oocytes indicates that the biophysical properties of the Para channel are similar to those of mammalian SCs (Warmke et al., 1997). Also, various toxins that act on mammalian SCs also act on Para, examples include permethrin and deltamethrin (Vais et al., 2001).

An ortholog of DSC1, BSC1, was cloned from the German cockroach, *B. germanica*. The sequence homology between BSC1 and DSC1 is high, 81%, 78%, 80%, and 88% in domains I, II, III, and IV, respectively (Liu et al., 2001). The functional expression of BSC1 in *Xenopus* oocytes revealed that the BSC1 channel is more permeable to Ca^{2+} than to Na^{+} and exhibits unique gating properties different from those of sodium channels, indicating that BSC1 encodes a Ca^{2+}-selective cation channel (Zhou et al., 2003, Liu et al., 2001). The functional analysis of DSC1 has not yet been published, however, personal communication with Dr. W. Song indicates that the DSC1 channel is also

calcium-selective and possesses gating properties similar to those of the BSC1 channel (Dr. W. Song, a postdoctoral associate in Dr. K. Dong's laboratory). In summary, DSC1 does not encode a sodium channel, and *para* is the only SC gene in insects.

V.B Conservation of Alternative Splicing of the Insect Sodium Channel Genes

Because of the involvement of SC mutations in pyrethroid resistance in many important insect and arachnid pest species, cDNAs (partial or full-length) of the SC gene have been isolated from many arthropod species (Soderlund, 2005). However, alternative splicing and RNA editing of the insect SC has mainly been studied in four insect species: *D. melanogaster, D. virillis, Musca domestica,* and *Blattella germanica.*

V.B1 *D. melanogaster:*

As mentioned previously, there exists a single SC gene, *para,* in D. *melanogaster* (Loughney et al., 1989; O'Dowd et al., 1989). Alternative splicing of *para* has been proposed to be the key mechanism influencing SC diversity (Loughney et al., 1989; O'Dowd and Aldrich, 1988; O'Dowd et al., 1995; Thackeray and Ganetzky, 1994, 1995; Warmke et al., 1997). Seven alternative exons (a, b, e, f, h, i, j) and four mutually exclusive exons (c/d and k/l) have been identified (Loughney et al., 1989; O'Dowd et al., 1995; Thackeray and Ganetzky, 1994, 1995; Warmke et al., 1997; Lee et al., 2002; Tan et. al., 2002a). The secondary structure of the insect SC along with the positioning of alternative splicing is presented in Figure 2.

In *D. melanogaster* alternative exons c, e, and f have been shown to be developmentally regulated. The percentage of transcripts in embryos containing exons c, e, and f were 1.7%, 3.4% and 87%, respectively, but changed to 24%, 28% and 6.7%, respectively in adults (Thackeray and Ganetzky, 1994).

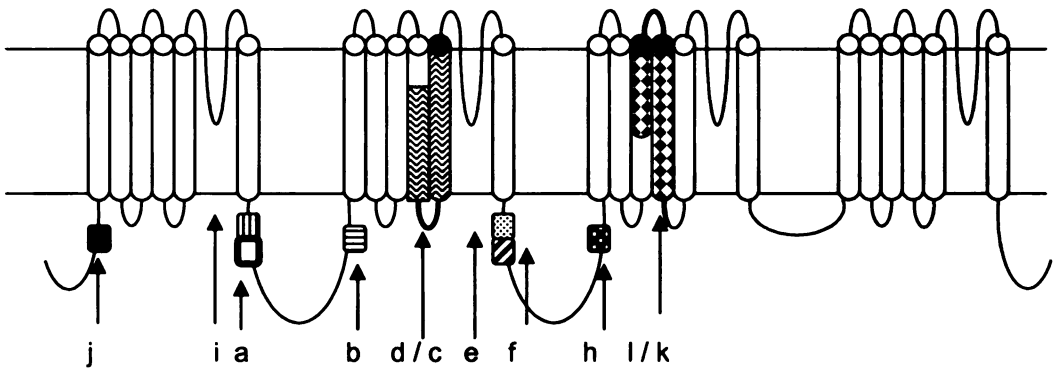

Figure 2. Topology of the insect SC containing positions of exons. Positions of sequences encoded by optional exons a, b, e, f, and h as well as mutually exclusive exons c and d in the sodium channel protein are highlighted in colored boxes. The letters below the boxes are the exons to which the boxes belong.

V.B2 *D. virilis*

The alternative exons of *para* identified in *D. melanogaster* are also found in *D. virilis* (Thackeray and Ganetzky, 1995). These alternative exons are highly conserved in amino acid sequence and are presented in Table 2 below. The protein sequence identities of the entire coding regions of *D. virilis* and *D. melanogaster* are 98.8% homologous, while the alternative exons are 99.5% homologous in amino acid structure (Thackeray and Ganetzky, 1995). Exons c, e, and f of *D. virilis* are developmentally regulated in a similar fashion to *D. melanogaster. D. virilis* embryos contain 0%, 9.2% and 70.2% exons c, e, and f, while adults contain 17.7%, 25%, and 11.3% respectively (Thackeray and Ganetzky, 1995). It was determined that 75% of *D. melanogasater* embryos and

57.3% of *D. virilis* embryos share the same exon usage; a+, b+, d, e-, f+ or a-, b+, d, e-, f+ (Thackeray and Ganetzky, 1994, 1995).

V.B3 *Musca domestica*

Like that of *D. melanogaster* and *D. virilis,* the *Musca domestica* (house fly) SC, Vssc1 (Voltage-sensitive sodium channel), contain exons a through h. In addition to these exons, two novel mutually exclusive exons k and l were identified in Vssc1. By searching the reported *para* sequence and performing a BLAST search exons k and l were subsequently identified in *para* (Lee et al., 2002). Exons b, f, h, and j of VSSC1 are identical in amino acid structure to Para, while exons a, d, e, and i have less than five changes and exon c has eight changes (Lee et al., 2002). Interestingly the regulation of alternative exons between *D. melanogaster* and *M. domestica* species is similar. Exons a, b, c, d, e, f, and i show comparable exon frequencies among the transcripts (Lee et al., 2002). The frequencies of exons h, j, k, and l among *para* transcripts have not yet analyzed.

V.B4 *Blattella germanica*

The cockroach SC, $BgNa_V$, is 78% and 76% identical in amino acid framework to Para and Vssc1 respectively (Dong, 1997). When comparing alternative exon sequences between *D. melanogaster, D. virilis, M. domestica,* and *B. germanica,* the sequences from *B. germanica* are quite divergent (refer to Table 3). Exon a of $BgNa_V$ contains fewer amino acids in comparison to exon a of *para*,, exon d is missing, and exons e, f, and i of $BgNa_V$ variants contain more amino acid changes than *D. virilis,* and *M. domestica* when compared to *para*. It

is interesting to note that the three fly sequences are more closely related to each other than with the cockroach sequence.

Three mutually exclusive exons have been identified in $BgNa_V$: G1, G2, and G3. G1 is equivalent to exon I of *para,* G2 corresponds to exon k of *para* and G3 is unique to $BgNa_V$, having not been identified in Para or other insect SCs. Exons G1, G2, and G3 of the cockroach are abundantly expressed in embryonic stages II and III, but were found in much lower frequencies in adults. Exon G1 is localized to the nerve cord, coxa and the remaining leg (femur, tibia, and tarsus). Exon G2 is the same as G1 but is expressed in the ovary and gut. Exon G3 is localized to the coxa and the remaining leg (Tan et al., 2002a).

V.C Alternative Splicing Generates Distinct Gating Properties of Insect Voltage-Gated Sodium Channels

Studies on mammalian SCs show that phosphorylation of protein kinase A (PKA) sites in the cytoplasmic linker connecting DI and DII modulates channel function (references in O'Dowd et al., 1995). The functional role of alternative splicing in para was initially investigated by O'Dowd and colleagues (O'Dowd et al., 1995).

Table 3. Alignment of the predicted amino acid sequences for optional exons a, b, e, f, h, i, and j and mutually exclusive exons c/d and k/l. Asterisks represent sequence homology and gaps were introduced for optimal alignment (dashes). The *para* and Vssc1 amino acid sequences were obtained from Lee et al., 2002, and correspond to GenBank accession #s M32078 and X96668, respectively. The *D. virilis* sequences (Thackeray and Ganetzky, 1994) corresponds to GenBank accession #s U26343 and U26722. The cockroach sequences were obtained from Song et al., 2004 and Tan et al., 2002, and correspond to the GenBank sequence U73583. Exon d has not been identified in $BgNa_v$ (Personal communication with Mrs. Nomura in Ke Dong's laboratory).

Table. 3 Amino acid sequence alignment of optional exons

a.	*Para*	TSLSLPGSPPNLRRGSRSSHK
	Vssc 1	**********I*********
	D. virilis	**********
	BgNav	A*****(a) [truncated exon]
b.	*Para*	VSVYYFPT
	Vssc 1	********
	D. virilis	********
	BgNav	**I******
c.	*Para*	LRVFKLAKSWPTLNLLISIMGRTVGALGNLTFVLCIIIFIFAVMGMQLFGKNYTD
	Vssc 1	**********VFYSVT
	D. virilis	**********
	BgNav	**********Y*
d.	*Para*	LRVFKLAKSWPTLNLLISIMGRTMGALGNLTPVLCIIIFIFAVMGMQLFGKNYHD
	Vssc 1	**********I*
	D. virilis	**********
	BgNav	
e.	*Para*	GERTNQISWINSE
	Vssc 1	***I*********
	D. virilis	***I*********
	BgNav	**--**S*-SWK*
f.	*Para*	-GKGVCRCISA
	Vssc 1	-**********
	D. virilis	-**********
	BgNav	DAHE—RDTDLDLT
h.	*Para*	MIGNSINHQDNRLEHELNGRGLSIQ
	Vssc 1	*******G**********H******
	D. virilis	******************H******
	BgNav	
i.	*Para*	VSVI-Q-RQPAPTTAHQAT-KVR-KVST
	Vssc 1	****-*-********P-**-***-****
	D. virilis	****-*-********P-**-***-****
	BgNav	VP*F*DTKTA*KS*F*FAYQENLVK
j.	*Para*	PRYGRKKKQKE
	Vssc 1	**********
	D. virilis	**********
	BgNav	GDF*****K**
k.	*Para*	LSLINLAAVWSGADDVPAFRSMRTLRALRPLRAVSRWEGMK
	Vssc 1	******V*****LN*IAV**********
	D. virilis	
	BgNav	********I*A**A*I**********R (G2)
l.	*Para*	VSLINFVASLVGAGGIQAFKTMRTLRALRPLRAMSRMQGMR
	Vssc 1	**********A**********
	D. virilis	
	BgNav	********** (G1)

O'Dowd and colleagues focused their study on exons a and i located along the same linker previously described to have PKA sites in mammalian SCs. Analysis of sodium current density in cultured embryonic neurons suggested that the presence of exon a was necessary for detection of sodium currents. They speculated that sodium current density is regulated by phosphorylation events because of a potential PKA site in exon a (O'Dowd et al., 1995). However, a later study investigating the role of exon a using *Xenopus* oocytes showed that the presence or absence of exon a did not alter expression of the sodium current (Warmke et al. 1997). To date, the functional consequence of exon a remains elusive.

The functional importance of exon b has been examined in $BgNa_v$ transcripts using the two-electrode voltage clamp system (Song et al., 2004). Deletion of exon b greatly enhanced the amplitude of sodium currents, whereas the inclusion of this optional exon dramatically reduced the amplitude of sodium currents in *Xenopus* oocytes. Interestingly, exon b contains a consensus sequence for phosphorylation that is hypothesized to serve as an on-off switch regulating neuronal excitability (Song et al., 2004).

Another study of cockroach SCs looked into the functional consequences of mutually exclusive exons G1, G2, and G3. Distinct gating and pharmacological properties were observed for transcripts containing G1 and G2, however, transcripts containing G3 were non-functional due to the addition of a stop codon. Transcripts containing exon G1 activate and inactivate at more hyperpolarized membrane potentials in comparison to transcripts containing exon G2. Channel sensivity to deltamethrin is greatly increased with the inclusion of

G1. Transcripts containing exon G2 have a 10-fold reduced sensitivity to deltamethrin than those containing G1 (Tan et al., 2002b).

V.D RNA Editing Generates Diversity in Insect Sodium Channels

RNA editing along with alternative splicing has been shown to generate molecular diversity in insect SCs. RNA editing is an important post-transcriptional modification that generates site-specific alterations of amino acids, in addition to insertions and deletions (references in Palladino et al., 2000a). A to I RNA editing is the result of deamination by the enzyme *Adar* (adenosine deaminase acting on RNA). This editase converts A to I through a process of hydrolytic deamination and has been reported to edit the SC in *Drosophila melanogaster*. Ten A to I RNA editing events have been identified in *Drosophila para* transcripts, and it appears that the frequency of editing events dramatically increase with age (references in Palladino et al., 2000a).

D. melanogaster mutants lacking Adar exhibit a variety of behavioral defects, providing profound evidence in support of the significance of A to I editing. Mutant larvae appeared normal in both locomotion and behavioral assays, while adults exhibit severe locomotion deficits and altered behavioral patterns. Abnormal behavioral phenotypes became increasingly acute with age. Tremors, strange body posture, slowness, difficulty mating, balance along with inefficient righting abilities, and circling behavior persistently worsened with age. Analysis of brain structure revealed brain lesions that intensified with age. Analysis of larval brains appeared normal while abundant lesions were present in adults. The extensive locomotive and behavioral defects seen in these mutants suggest

that ADAR editing events in the nervous system are necessary to perform normal function (Palladino et al., 2000b).

In the German cockroach, *B. germanica,* A to I and U to C RNA editing of $BgNa_V$ has been reported. Similar to that of alternative splicing, tissue-specific and developmental-specific regulation of these RNA editing events has also been documented (Song et al., 2004). Two described U to C RNA editing events in $BgNa_V$ undergo tissue-specific regulation; a leucine to proline change in DIIIS1 and a valine to alanine change in DIVS4. The tissues of ovary, gut, nerve cord, and leg were analyzed and both changes were found to only occur in the first two tissues listed (Song et al., 2004). Enzymes that catalyze or mediate U to C editing have not yet been identified. Also, an A to I editing event resulting in an isoleucine to methionine change in DIVS4 is regulated in a tissue specific manner. Transcripts of this A to I editing event were isolated from nerve cord and leg (Song et al., 2004).

In addition to tissue-specific regulation, the A to I editing of DIVS4 is also developmentally regulated. Only the unedited transcript was found in the embryonic stage I while both edited and unedited were detected in two embryonic (II and III) and two immature (nymph I and II) stages.

V.E Electrophysiological Analysis of RNA Edited Variants of $BgNa_V$

RNA editing of $BgNa_V$ along with alternative splicing produces SCs with distinct gating properties (Tan et al., 2002a; Liu et al., 2004, Song et al., 2004). Changes in current, activation, and inactivation are among some of the obvious results of RNA editing events. Examples include a U to C modification resulting in an F to S change at the C-terminal domain that was found to impair

inactivation resulting in persistent current. It is speculated that the C-terminal domain interacts with the IFM motif or docking receptor (discussed earlier) and modulates the kinetics of inactivation (Liu et al., 2004). An A to I editing event resulting in a lysine to arginine change in D1S2 causes a depolarizing shift in the voltage-dependence of activation by nearly seven millivolts (Song et al., 2004). To date, RNA editing events of the insect SC have only been documented and functionally characterized in the cockroach system. The U to C and A to I RNA editing events previously mentioned are the only two editing events that have been demonstrated to confer altered gating properties. RNA editing could be a major mechanism for increasing the diversity of sodium channel function. More research in this area needs to be done in order to characterize the importance of RNA editing and to understand the physiological roles it may play.

VI. Pharmacology of Voltage-Gated Sodium Channels

Sodium channels are integral transmembrane proteins responsible for the rising phase of action potentials (Catterall, 2000). Because of their fundamental role in neural excitability they are a target site of neurotoxins produced by animals and plants for defense and preying strategies as well as therapeutic drugs (Wang and Wang, 2003). Binding of toxins to SCs change normal channel functional and can result in modifications ranging from blocking the channel pore to altering normal activation and inactivation processes (Wang and Wang, 2003). These toxins are grouped into nine types according to their distinct effects and receptor sites on the sodium channel (Table 4). The molecular determinants of receptor sites one through five, seven, and nine have been identified (Table 4).

Table 4: Neurotoxins that act on sodium channels

Receptor Site	Neurotoxins	Physiological Effects	Location
1	Tetrodotoxin saxitoxin μ-conotoxin	Binds to extracellular pore; block Na^+ ion entry	S5-6 loop of D1, D2, D3, D4
2	Batrachotoxin veratridine grayanotoxin	Persistent activation	Segment 6 of D1, D2, D3, D4
3	α-scorption toxins sea anemone toxins	Block Inactivation	S3-4 loop of D4 S5-6 loop of D1, D4
4	β-scorpion toxins	Prolong activation, hyperpolarized shift of activation	S1-S2 loop of D2 S3-S4 loop of D2
5	Brevetoxins ciguatoxins	Persistent Activation	Segment 6 of D1 Segment 5 of D4
6	б-conotoxins	impair Inactivation	Unknown
7	DDT, pyrethroids	Block activation depolarized shift of resting potential	Segment 6 of D1, D2, D3
8	Conus stratius toxin	Prolong activation	Unknown
9	Local anesthetics,	Block Inactivation, prevent ion entry	Segment 6 of D1, D2, D3

Modified from Wang and Wang (2003).

The most relevant toxin this study is LqhαIT, an alpha scorpion toxin extracted from *Leiurus quinquestriatus hebraeus*. Alpha scorpion toxins bind to receptor site three and remove fast inactivation resulting in prolonged sodium ion entry into the cell (Gordon et al., 1996). These neurotoxins are classified into

four groups based on pharmacological properties and structural similarities (Gordon et al., 1996). The 'classical' alpha scorpion toxins are highly active on mammalian SCs and weakly active on insect SCs. The prototype for classical alpha scorpion toxins is AaH II because of its high affinity towards mammalian brain synaptosomes (Gordon et al., 1996). Those toxins that are weakly toxic to both insects and mammals are represented by Lqq IV. These toxins competitively inhibit the binding of AaH II in mammalian systems as well as LqhαIT in insect SCs (Gordon et al., 1996). "Alpha-like scorpion toxins' are active on both mammalian and insect SCs. Interestingly though, alpha-like toxins Bom III and Bom IV compete with LqhαIT for binding on insect SCs, but not AaH II of mammalian VGSCS. However, because of their "classical" inhibition of inactivation and competitive binding with LqhαIT, they are termed 'alpha-like'. Those toxins that are highly toxic to insects and weakly toxic to mammals are considered insect-selective. LqhαIT is significantly more toxic to insect SCs than to mammalian SCs (Gordon et al., 1996).

The α-scorpion toxins are small polypeptides of 63 to 70 amino acids cross-linked by four disulfide bridges (Cestele and Catterall, 2000). LqhαIT is greater than ten fold more active against insect SCs than mammalian SCs (Lee et al., 2000). Because the effect of LqhαIT binding to insect SCs resembles the classical scorpion toxins suggests that the receptor site on insect SCs would be similar to mammalian SCs. However, because LqhαIT exhibits selective tendencies towards insect sodium channels and not mammalian sodium channels indicates that there are unique structural features of the insect sodium channel that confers selective binding. It has been proposed that there are

distinct but overlapping receptor sites in insect and mammalian SCs for the binding of mammalian- and insect-selective toxins (Gordon et al.,1996). While photoaffinity labeling, site-directed mutagenesis studies, and site-directed antibodies against individual extracellular loops revealed DIS5-S6, DIVS5-S6, and DIVS3-S4 are involved in alpha-scorpion toxin binding on mammalian sodium channels (references in Rogers et al., 1996), the critical amino acid residues involved in the binding to insect SCs have not been identified.

CHAPTER 2: Specific Aims, Rationale, and Significance

Specific Aims:

The long-term goals of this project are to understand the functional diversity of insect voltage-gated sodium channels (SCs); to elucidate the molecular interactions between SCs and neurotoxins particularly insecticides; and to understand the biological role of alternative splicing and RNA editing of insect SC genes. The specific objectives of my masters thesis project are:

Objective 1. Expression and functional characterization of all 64 Para variants using a two-electrode voltage clamp / *Xenopus* oocyte expression system.

Objective 2. Pharmacological analysis of the functional sodium channel variants using the α-scorpion toxin, LqhαIT.

Rationale and Significance of Objectives:

There exists one gene encoding SCs in insects. Transcripts of this gene undergo extensive alternative splicing and RNA editing events, generating functionally and pharmacologically distinct sodium channels. A single composite full-length clone of para is currently available for functional, pharmacological, and molecular analysis. This clone was constructed by ligating two overlapping cDNA fragments (Warmke et al., 1997), and may not represent a true splice type or the variety of sodium channels *in vivo*.

Dr. Zhiqi Liu, a postdoctoral associate in Ke Dong's laboratory, isolated sixty-four full-length clones of *para* by RT-PCR of the entire coding region. It is likely that these clones represent a suite of *in-vivo* splice types. Sequence analysis of the full-length clones should reveal novel alternative splicing and RNA editing sites. Comparison of alternative exon use and RNA editing events between *para* and German cockroach SC genes would aid in the identification of common and distinct features of these events. Expression and functional analysis of the full-length cDNA clones in *Xenopus* oocytes is likely to reveal Para variants with unique gating properties similar to and differing from the properties previously identified in the German cockroach SCs (Tan et al., 2002; Song et al., 2004; Liu et al., 2004). This information will be the foundation for future experiments that will outline the importance of RNA editing and alternative splicing *in vivo* by taking advantage of the unique genetic tools available only in *D. melanogaster*.

The SC is the primary target of various neurotoxins, including insecticides. Sodium channels exhibit distinct pharmacological profiles in both insect and mammals (Zhao et al., 2005; Song et al., 2006). This thesis will focus on the alpha scorpion toxin, LqhαIT for pharmacological analysis. LqhαIT is an insect-specific scorpion toxin and little is known pertaining to the binding site of LqhαIT on insect SCs. The response of Para variants to LqhαIT application will be determined. Identification of LqhαIT susceptible and resistant variants will provide valuable resources towards the analysis of molecular determinants that are critical for toxin binding and action.

CHAPTER 3: Functional and Pharmacological Characterization of Sixty-Four Para Sodium Channel Variants in *Xenopus* Oocytes

ABSTRACT

Extensive alternative splicing and RNA editing of the *Drosophila melnaogaster* voltage-gated sodium channel (SC) gene, *para,* has been documented. However, the functional consequences of these post-transcriptional modifications have not yet been investigated. In this study we report the isolation, expression, and functional characterization of sixty-four full-length *para* cDNA clones. The sixty-four clones were grouped into twenty-nine splice types based on alternative exon usage. Functional analysis of these variants revealed a broad spectrum in the voltage-dependence of activation with the voltages for half-maximal activation ranging from -6.8 mV to -46.8 mV. The voltage dependence of inactivation, however, was less variable. Sequence comparison of three functionally distinct variants uncovered three novel A to I editing sites. Furthermore, we revealed differential sensitivities of these variants to LqhαIT, an *α*-scorpion toxin isolated from *Leiurus quinquestriatus hebraeus*. The observed functional and pharmacological diversity of *para* variants supports the notion that alternative splicing and RNA editing are the two major mechanisms for generating sodium channel diversity in insects.

INTRODUCTION

Voltage-gated sodium channels (SCs) are integral transmembrane proteins responsible for the generation of action potentials across the membranes of excitable cells. The mammalian SC consists of a large, membrane bound, pore-forming, voltage-sensing α-subunit of approximately 260 kDa, along with several smaller auxiliary β subunits. The α-subunit is composed of four repeated homologous domains (I-IV), each containing six hydrophobic transmembrane segments (S1-S6). Mammals have nine genes that encode for functionally and pharmacologically distinct SCs each with unique tissue, developmental, and cellular-specific expression patterns (see Chapter 1 for details; review by Catterall, 2000).

Insect SCs, unlike mammalian counterparts, are encoded by a single gene. The *Drosophila melanogaster* SC, *para,* was isolated from temperature-sensitive paralytic mutants using P-element transposon tagging (Loughney et al., 1989). The complete Para amino acid sequence was deduced from six overlapping cDNA clones and was predicted to have extensive homology (greater than 58 percent for each four domains) to mammalian SCs (Loughney et al., 1989). Alternative splicing and RNA editing of *para* are predicted to be two major mechanisms for increasing molecular and functional diversity of insect SCs (Loughney et al., 1989; O'Dowd and Aldrich, 1988; O'Dowd, 1995; Thackeray and Ganetzky, 1994, 1995; Warmke et al., 1997; Palladino et al., 2000), but, the functional consequences of alternative exons and RNA editing sites have not been determined in *para*. However, the importance of alternative splicing and RNA editing of the German cockroach SC gene $BgNa_V$ in creating insect SC

functional diversity has been recently documented (Tan et al., 2002a; Liu et al., 2004; Song et al., 2004).

Prior to our study a single variant of *para* has been functionally characterized in *Xenopus* oocytes (Warmke et al., 1997). However, this composite full-length cDNA clone may not represent a splicing type *in vivo* because it was constructed by ligating two overlapping partial cDNA clones. In this study we report the isolation, expression, functional and pharmacological characterization of sixty-four full-length *para* cDNA clones.

MATERIALS AND METHODS

Synthesis of first strand cDNAs

Total RNA was isolated using Invitrogen TRIzol Reagents (Invitrogen, Rockville, MD). Isolation of mRNA was performed using Promega polyA+ RNA isolation kit (Promega, Madison, WI). First-strand cDNA was synthesized from mRNA using a Para-specific primer (D-3'-1; 5' – TAC TCA TGC TAA TAC TCG CG -3') based on the sequence of a region immediately down stream of the stop codon (Genbank accession M32078), and SuperScript II RNase H-reverse transcriptase (Invitrogen, Rockville, MD). First strand cDNA synthesis reaction conditions were: incubation at 42°C for 2 min. followed by a 60 min. incubation at 48°C. RNA was removed using RNaseH followed by a 20 min. incubation at 37°C.

PCR and cloning of *para* full-length cDNAs

To amplify the entire coding region of para (6 kb) by PCR, a forward primer (D-para-KpnI - 5'–CGG GGT ACC GCC ACC ATG GCA GAA GAT TCC GAC TCG-3') and a reverse primer (D-para-Xba - 5'–GCT CTA GAT ACT GCT

AAT ACT CGC G–3') were designed based on the 5' and 3' sequences of the *para* open reading frame. Xba and KpnI restriction enzyme site sequences (underlined) were added to the forward and reverse primers, respectively, to facilitate cloning. A Kozak sequences (double underlined) was added to the primer D-para-KpnI for high-efficiency translation. The reaction mixture of amplification (50 μl) contained 0.5 μl cDNA, 50 pmol each of primers D-para-Xba and D-para-KpnI, 200 μM each dNTP, 1 U eLONGase (Invitrogen), 1.5 mM $MgCl_2$, and 1X PCR reaction buffer. PCR amplification was carried out as follows: 1 cycle of 94° C for 1 min.; 33 cycles of 94° C for 30 sec., 58° C for 30 sec., 68° C for 8 min.; one cycle of 68° C for 15 min. The PCR products were purified using QIAEX II Gel Extraction Kit (QIAGEN Sciences, Maryland) and cloned in pGH19, an oocyte expression vector. Plasmids were transformed into competent bacterial cells, Stbl2 (Invitrogen), and sixty-four positive colonies were isolated.

Expression of *para* sodium channels in *Xenopus* laevis oocytes

Oocytes were obtained surgically from oocyte-positive female *Xenopus laevis* (Nasco, Ft. Atkinson, WI). Females were anesthetized with Tricaine (3-aminobenzoic acid ethyl ester) at 2g/liter, and several lobes of the ovary were surgically removed. Follicle cells surrounding the oocytes were loosened by collagenase treatment (1mg/ml Type 1A collagenase, Sigma Co., St. Loise, MO) in calcium-free ND-96 medium (96 mM NaCl, 2mM KCl, 1 mM $MgCl_2$, and 5 mM HEPES adjusted to a pH of 7.5) then the remaining follicle cells were removed with forceps. Isolated oocytes were incubated in ND96 medium (96 mM NaCl, 2mM KCl, 1 mM $MgCl_2$, and 5 mM HEPES, 1.8 mM $CaCl_2$, 50 μg/ml gentamicin,

5mM pyruvate, and 0.5 mM theophylline, adjusted to a pH of 7.5) (Goldin, 1992). Healthy oocytes stages V and VI were used for cRNA injection.

Plasmid DNAs containing the *para* and TipE (auxiliary subunit of the *para* construct, refer to Chapter 1 for details) constructs were linearized by *NotI*. cRNAs were prepared by *in vitro* transcription with T7 polymerase (mMESSAGE mMACHINE kit, Ambion). TipE and para cRNAs were co-injected (0.25 ng – 10 ng) into *Xenopus* oocytes. TipE facilitates robust expression of para current in oocytes (see Chapter 1 for details). Oocytes with peak sodium current of 0.5 μA-2 μA were used for functional analysis using the two-electrode voltage clamp. Usually 0.5 μA- 2 μA of sodium current can be detected in the oocyte one to five days following cRNA injection. Typically, by the sixth day, the oocyte condition was too poor for recording currents.

Electrophysiological recording and analysis

Sodium currents were recorded using a standard two-electrode voltage clamp system (Kontis and Goldin, 1993). Voltage and current borosilicate glass electrodes were filled with 3 M KCl and manipulated for a resistance of less than 0.5 MΩ. Amplifier OC725C (Warner Instrument Corp. Hamden CT), Digidata 1320A, and pCLAMP 8.2 software (both of Axon Instrument, Foster City, CA) were used for current measurement. All experiments were performed at room temperature (20 to 22°C). Capacitive transient and linear leak currents were corrected using the P/N subtraction technique.

The voltage-dependence of conductance (G) was calculated by measuring peak currents at test potentials ranging from -80 to +65 mV in increments of 5 mV and dividing by $(V-V_{rev})$, where V is the test potential and V_{rev} is the reversal

potential for sodium. Reversal potentials were determined from the I-V curves and peak conductance values were normalized to the maximal peak conductance (G_{max}). Peak conductance values were fitted with a Boltzmann equation of the form $G=1-[1+\exp(V-V_{1/2})/k]^{-1}$. Where V is the potential of the voltage pulse, $V_{1/2}$ is the half-maximal voltage for activation, and k is the slope factor.

The voltage-dependence of inactivation was determined using 200ms inactivating prepulses ranging from -120 mV to -15 mV in 5 mV increments from a holding potential of -120 mV. Peak current amplitude during the test depolarization was normalized to the maximum current amplitude, and plotted as a function of the pre-pulse potential. The data were fit with a Boltzman equation of the form $I=I_{max}*[1+(\exp(V-V_{1/2})/k)]^{-1}$, where I_{max} is the maximal current, V is the voltage pulse potential, $V_{1/2}$ is the voltage at which half of the current is inactivated, and k is the slope factor.

LqhαIT sensitivity assay

LqhαIT was generously provided by M. Gurevitz (Tel Aviv University, Israel). The method used for application of LqhαIT in the recording system is identical to that described by Tan et al. (2002). Briefly, disposable recording chambers were made in Petri dishes with hot glue dams (1-1.5 ml volume). LqhαIT was delivered to the oocyte recording chamber by hydrostatic force using glass capillary tubes. The toxin-induced effects were quantified by the ratio of the current amplitude 20 ms into depolarization (I_{20}) over the peak current (I_{peak}).

RESULTS

Molecular analysis of 64 full-length cDNA clones

Prior to our study, eleven alternative exons were identified in the *para* transcript (Thackeray and Ganetzky, 1994; O'Dowd et al., 1995; Warmke et al., 1997; Lee et al., 2002). Seven of them are optional (a, b, e, f, h, i, j), and four are mutually exclusive (c/d and l/k; Fig.1A). In this study, Dr. Zhiqi Liu isolated sixty-four para full-length cDNA clones using RT-PCR. Determination of the alternative exon usage in these variants was done by using PCR or sequencing. Our analysis revealed twenty-nine splice types (Fig. 1B). The most abundant splice type is

a, b, d, i, j, l. It is interesting that out of seven optional exons and four mutually exclusive exons that only twenty-nine splicing types were observed because there is a possibility of forming 20,160 splicing types. Most of the variants contain exons a, d, i, j, l suggesting that there is selection pressure for these exons.

Functional expression of 64 variants in *Xenopus* oocytes

All sixty-four of the *para* variants were co-injected with TipE into *Xenopus* oocytes for functional analysis using the two-electrode voltage clamp expression system. Twenty-six of the variants did not generate any sodium current even eight days after cRNA injection. Another six variants produced detectable sodium currents, but the currents were too small (less than 0.5 μA) for functional analysis. Sodium currents from the remaining thirty-two variants were sufficient for functional analysis (0.5 μA -2 μA). We determined the voltage-dependence of activation and inactivation of these thirty-two variants.

As presented in Table 1, the voltages for half maximal activation ($V_{1/2}$) varied greatly among the functional constructs. We divided the variants into three groups based on their voltage dependence of activation. Five variants, 50, 55, 48, 32, and 53, required more positive membrane potentials for activation with a $V_{1/2}$ of -6.8 mV to 15.69 mV and were designated as high-voltage activated (HVA) variants. Nine variants, 49, 10, 45, 27, 62, 22, 2, 21, and 18, activated at more negative membrane potentials with $V_{1/2}$ of -26 mV to -46 mV, and were termed low-voltage activated (LVA) variants. The majority of the variants had a $V_{1/2}$ value of -20 mV to -25 mV, and were labeled mid-voltage activated (MVA) variants. Voltages for half maximal inactivation ($V_{1/2}$) were less variable for most of the variants with a range of -32 mV to -50 mV. Variant 18 was unique in that it inactivated at strongly hyperpolarized potentials (-65 mV) and also activated at extremely hyperpolarized potentials (-47 mV).

Sequence analysis of three functionally distinct variants

Three *para* variants were sequenced, each representing one of the three activation groups; LVA (variant 18), MVA (variant 13), and HVA (variant 50). Each variant contained unique alternative splicing and RNA editing sites. Variant 13 belonged to splice type fourteen (c, i, j, l), variant 18 belonged to splice type seven (a, c, j, l), and variant 50 belonged to splice type nineteen (d, e, f, i, j, k).

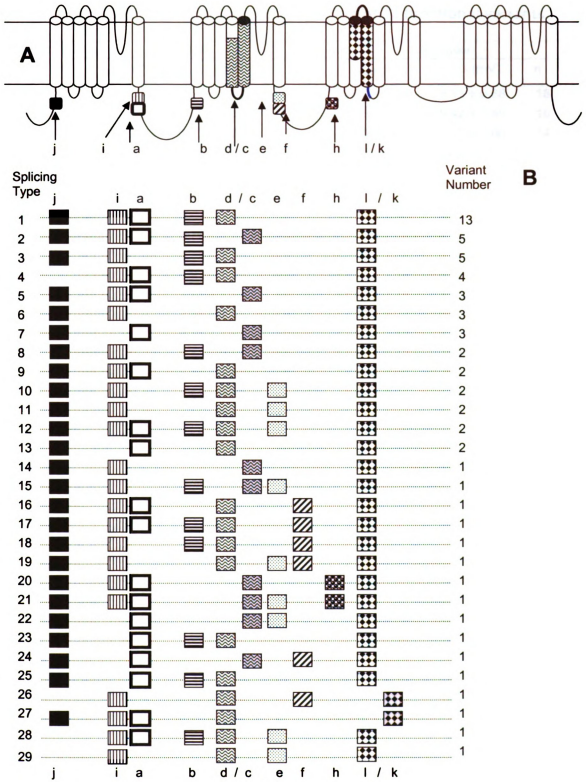

Figure 1. Identification of 29 splice types. **A.** A topological view of the sodium channel with positions of alternative exons indicated by colored boxes (A). **B.** Schematic presentation of alternative exon usage in each splice type.

Table 1. Activation and inactivation properties of 32 functional variants.

Variant	Activation			Inactivation		
	$V_{1/2}$ (mV)	k (mV)	n	$V_{1/2}$ (mV)	k (mV)	n
50	-6.80 ± 1.74	5.20 ± 1.10	12	-50.83 ± 1.69	6.11 ± 0.68	18
55	-9.94 ± 3.72	9.39 ± 4.56	6	-50.19 ± 2.95	5.42 ± 0.85	10
48	-11.42 ± 2.34	7.33 ± 0.79	14	-34.90 ± 3.86	5.47 ± 1.06	14
32	-14.78 ± 3.24	7.27 ± 0.96	21	-42.32 ± 5.22	7.31 ± 6.20	39
53	-15.69 ± 2.05	8.16 ± 1.06	10	-45.46 ± 1.30	7.46 ± 0.63	12
28	-19.37 ± 1.81	6.88 ± 1.20	20	-39.81 ± 2.88	6.06 ± 1.50	37
38	-20.49 ± 4.63	7.94 ± 1.37	8	-46.72 ± 0.46	4.84 ± 0.55	7
17	-20.57 ± 2.72	6.78 ± 1.31	13	-46.38 ± 2.69	4.98 ± 0.43	18
58	-21.60 ± 2.68	6.33 ± 1.22	23	-40.99 ± 2.02	5.28 ± 0.65	24
24	-21.60 ± 2.07	6.90 ± 1.19	21	-43.95 ± 2.14	5.36 ± 0.72	25
7	-22.40 ± 2.48	7.44 ± 1.19	11	-47.41 ± 2.78	5.12 ± 0.70	15
19	-22.29 ± 3.07	8.68 ± 1.57	19	-45.39 ± 2.27	5.44 ± 0.79	25
11	-22.71 ± 3.75	8.11 ± 1.83	19	-47.32 ± 2.12	5.55 ± 0.42	23
13	-22.74 ± 3.33	3.46 ± 0.64	11	-32.07 ± 2.17	3.85 ± 0.49	17
39	-23.26 ± 4.58	5.49 ± 1.54	19	-39.87 ± 2.90	5.29 ± 1.10	13
41	-23.70 ± 3.33	4.50 ± 0.83	24	-40.09 ± 2.65	4.54 ± 1.01	24
24	-23.77 ± 3.72	6.69 ± 0.85	14	-48.31 ± 2.30	5.32 ± 0.48	15
31	-24.03 ± 2.98	5.15 ± 0.80	12	-45.06 ± 1.97	4.83 ± 0.74	22
47	-25.34 ± 4.34	4.70 ± 1.25	20	-42.87 ± 2.59	4.82 ± 0.33	20
57	-25.66 ± 2.23	5.80 ± 1.23	3	-46.07 ± 3.08	4.87 ± 0.36	15
56	-25.72 ± 4.06	5.94 ± 1.39	20	-35.05 ± 3.09	4.94 ± 0.42	21
8	-25.75 ± 1.95	6.38 ± 1.58	8	-47.11 ± 2.20	4.92 ± 0.33	11
44	-25.99 ± 4.49	3.00 ± 1.30	24	-39.21 ± 1.46	4.18 ± 0.44	24
49	-26.25 ± 2.66	5.08 ± 1.01	17	-43.51 ± 1.59	4.85 ± 0.30	19
10	-26.33 ± 5.77	3.95 ± 1.19	18	-38.95 ± 1.64	4.84 ± 0.51	19
45	-27.13 ± 3.80	5.81 ± 1.04	24	-45.15 ± 2.64	5.35 ± 0.21	24
27	-27.16 ± 3.92	4.91 ± 1.13	21	-41.86 ± 3.18	5.02 ± 0.30	22
62	-29.08 ± 3.58	3.68 ± 0.87	17	-42.88 ± 1.82	4.49 ± 0.37	18
22	-29.53 ± 2.48	10.36 ± 2.07	13	-49.19 ± 1.95	6.48 ± 1.19	13
2	-29.67 ± 7.27	4.35 ± 1.19	33	-42.01 ± 2.45	5.05 ± 0.52	37
21	-31.66 ± 3.69	4.32 ± 0.90	20	-43.66 ± 2.07	4.55 ± 0.29	25
18	-46.56 ± 4.55	6.17 ± 1.06	17	-65.42 ± 2.42	4.43 ± 0.46	24

Sequence comparison of variants 13, 18, and 50 with the GenBank Para sequence (accession number M32078) revealed fifteen, twelve, and eight amino acid changes, respectively (Figure 2 and Table 2). In an earlier study, ten A to I

editing sites were identified in *para* (Palladino et al., 2000a). Five of the observed changes from this study match five of the previously reported A to I editing sites (Palladino et al., 2000). Because PCR mistakes are unlikely to occur in multiple variants, we have identified and additional three A to I editing sites (observed in multiple variants; Table 2A). Additionally, two nucleic acid changes were observed in multiple variants that resulted in a guanine to cytosine change. However, whether these are the result of alternative splicing or a novel type of RNA editing remains to be determined.

Nucleic acid changes that occur in a single variant may be the result of RNA editing, alternative splicing, or a mistake made during PCR. Fifteen distinct nucleic acid changes were observed in variants 13, 18, and 50 (Table 2B). One of these changes, N1822S, corresponds to a previously recognized A to I editing site (Palladino et al., 2000a). The remaining fourteen changes need to be further investigated to determine the foundation of change.

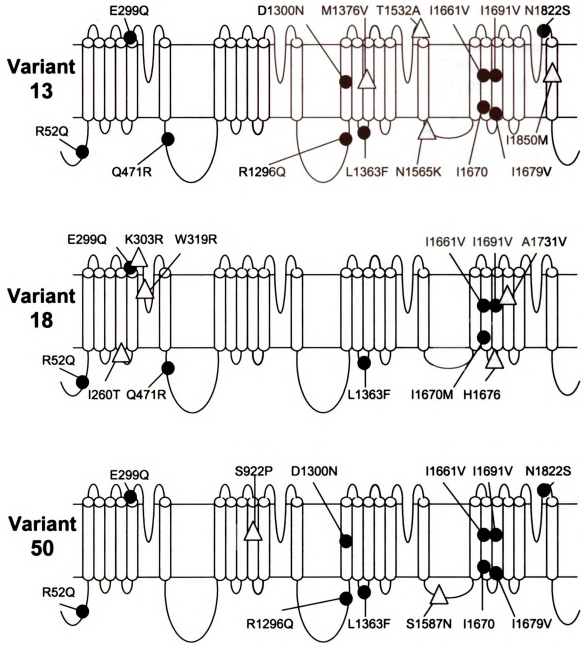

Figure 2. Amino acid changes in variants 13, 18, and 50. The secondary structure of variants 13, 18, and 50 along with the position of amino acid change compared to the GenBank sequence (M32078). For example, R52Q indicates R in the Genebank sequence and Q in variants at the amino acid position 52. Amino acid changes occur in more than one variant are indicated by the darkened circles. Triangles represent variant-specific amino acid changes.

Table 2. Amino acid changes observed in variants 13, 18, and 50.

Variant 13	Variant 18	Variant 50	Nucleo-tide Change	Location	RNA Editing Type	Report-ed A to I
A						
R 52 Q	R 52 Q	R 52 Q	g-a	N.T.	A to I	*
E 299 Q	E 299 Q	E 299 Q	g-c	IS5-IS6	?	
Q 471 R	Q 471 R		a-g	I-II	A to I	*
R 1296 Q		R 1296 Q	g-a	II-III	A to I	*
D 1300 N		D 1300 N	g-a	IIIS1	A to I	*
L 1363 F		L 1363 F	g-c	IIIS2-IIIS3	?	
I 1661 V	I 1661 V		a-g	IVS1-IVS2	A to I	
I 1670 M	I 1670 M		a-g	IVS2	A to I	
I 1691 V	I 1691 V		a-g	IVS3	A to I	
B						
	I 260 T		a-g	1S4-1S5		
	K303R		a-g	IS4-IS5		
	W319		t-c	IS5-IS6		
		S 922 P	t-c	IIS4		
	L1363F		g-c	IIS2-IIS3		
M 1376 V			a-g	IIIS3		
		Q 1450 R	a-g	IIIS5		
T 1532 A			a-g	IIIS5-IIIS6		
N 1562 K			t-g	III-IV		
		S 1587 N	g-a	III-IV		
	H1676R		a-g	IVS2-IVS3		
I 1679 V			a-g	IVS3		
	A 1731 V		c-t	IVS4		
N 1822 S			a-g	IVS5-IVS6		*
I 1850 M			a-g	IVS6		

Note: N.T. represents the N-terminal domain. Question marks (?) indicate that the mechanism underlying the amino-acid changes are unknown. Asterisks (*) represent the previously reported A to I editing sites in *para* (Palladino et al., 2000).

Examination of the sensitivity of Para variants to LqhαIT

LqhαIT, an alpha scorpion toxin isolated from *Leiurus quinquestriatus hebraeus,* binds to receptor site three (refer to Chapter 1) and removes fast inactivation resulting in prolonged action potential propagation (Chen et al.,

2000). LqhαIT is polypeptide of 66 amino acids that is ten fold more selective to insect SCs than to mammalian SCs (Lee et al., 2000).

To examine the sensitivities of the functional variants of *para* to 1 nM LqhαIT, we determined the ratio of I_{20}/I_{peak} before and after toxin application (Figure 3; Table 3). Although inactivation was affected by 1 nM LqhαIT for all variants, some variants are more sensitive than others. For example, variant 21 is most resistant to LqhαIT compared to all other variants with only 29% of inactivating current inhibited by 1 nM LqhαIT. Variants 8 and 58 are among the most sensitive ones with inactivation being completely abolished by toxin application. To quantitatively compare the effect of LqhαIT between variants 8 and 21, dose-response curves were created (Fig. 4). While the EC_{50} of variant 8 could not be generated due to an inadequate number of data points, Figure 4 indicates that variant 8 is apparently more sensitive than variant 21 (EC_{50} of 2.58 nM) to LqhαIT.

Table 3. Effects of 1 nM LqhαIT on *para* variants

Variant	I_{20}/I_{peak} (%) ± SD	n	Variant	I_{20}/I_{peak} (%)± SD	n
21	29 ± 13	12	19	62 ± 18	3
62	34 ± 13	4	55	66 ± 22	3
2	58 ± 33	27	13	78 ± 36	13
10	34 ± 13	4	11	79 ± 16	3
22	34 ± 13	4	8	80 ± 25	18
47	29 ± 13	12	17	81 ± 9	4
56	34 ± 13	4	50	85 ± 37	2
39	58 ± 33	27	7	86 ± 12	2
48	60 ± 15	6	31	88	1
18	61 ± 17	6	44	88	1
25	56 ± 14	5	27	93	1
45	58	1	24	94 ± 1	4
49	58	1	52	105 ± 7	8
41	59 ± 0	2	32	105	1
57	62 ± 27	4	58	105 ± 9	2

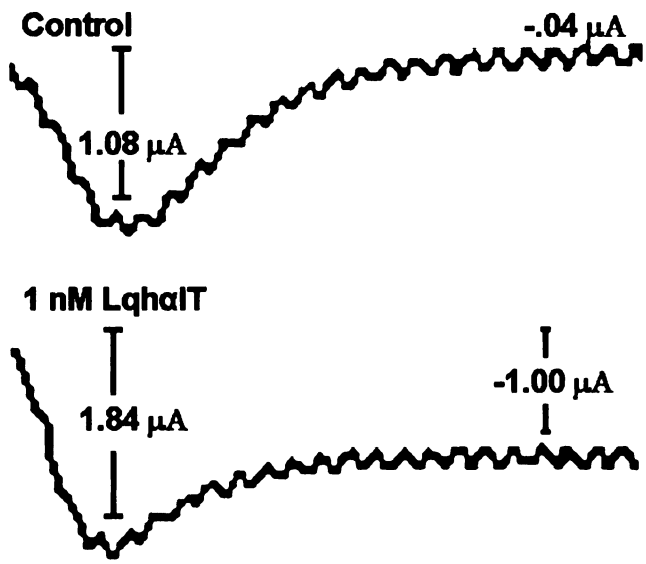

Figure 3. Peak sodium current traces of variant #8 before and after application of 1 nM LqhαIT. Peak current was measured by depolarizing the oocytes membrane to -10 mV for 20 ms from a holding potential of -120 mV. Peak current was determined before the application of 1 nM LqhαIT and ten minutes after the application of 1 nM LqhαIT.

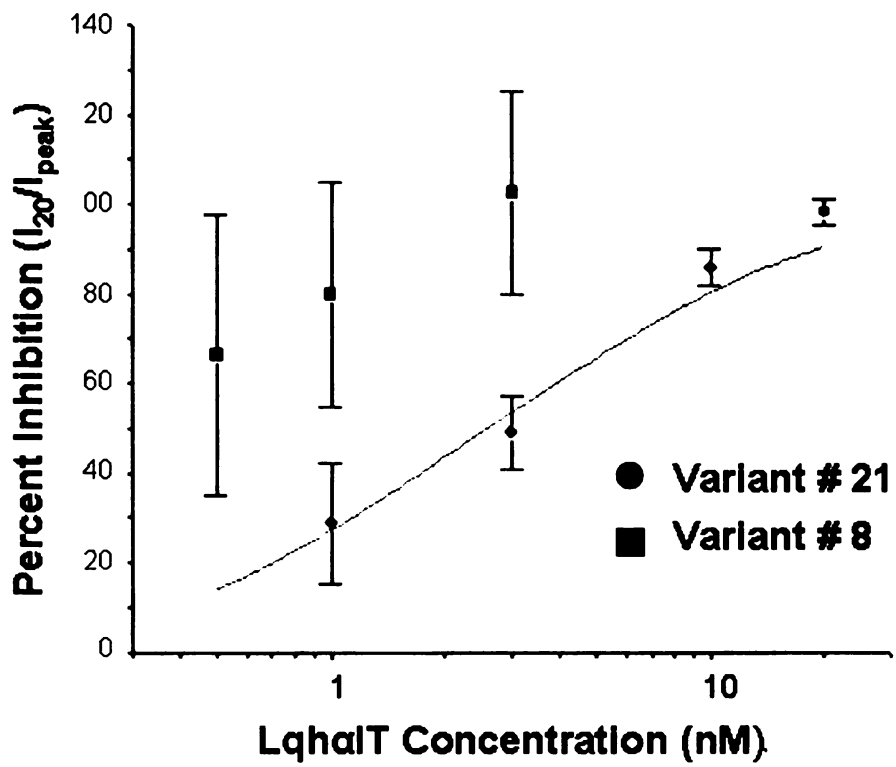

Figure 4. Dose response curves of variants 8 and 21. Dose–response curves were fit with a Hill equation of the form $y = V_{max} [x^n/(k^n + x^n)]$. Variant 21 has an EC_{50} of 2.58 nM. More data points were needed to determine the EC_{50} of variant 8.

Variants 8 and 21 were selected for sequence analysis because of their differential sensitivities to LqhαIT. The results of this analysis are presented in Figure 5 and Table 4. Eight of the observed changes correspond to the previously recognized RNA editing sites. Three of the changes are identical to the earlier mentioned possible RNA editing sites and five are novel. Variant 8 has one novel amino acid change (K1455R) and variant 21 has two novel amino acid changes (I1519V and H1772Y) that are located on the extracellular loops of the pore and that may interact with the binding of LqhαIT.

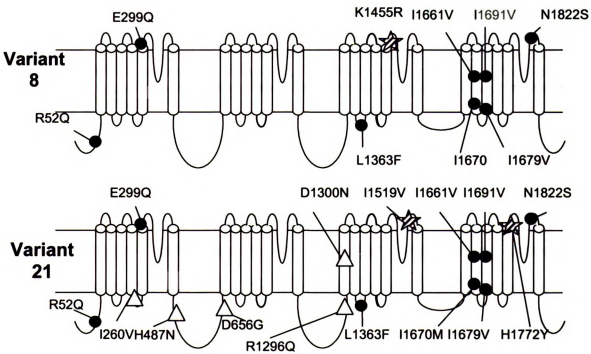

Figure 5. Amino acid changes in variants 8 and 21 compared to GenBank # M32078. This figure depicts the topology of variants 8 and 21. Circles indicate common changes. Triangles represent unique changes in the transmembrane regions, and stars indicate unique changes in the extracellular portion.

Table 4. Sequence comparison of variants 8 and 21

Variant 8	Variant 21	Nucleotide Change	Location
R 52 Q[1]	R 52 Q[1]	g-a	N.T.
	I 260 V[2]	a-g	IS4-S5
E 299 Q[1]	E 299 Q[1]	g-c	IS5-IS6
	H 487 N[3]	c-a	IS6-IIS1
	D 656 G[3]	a-g	IS6-IIS1
	R 1296 Q[1]	g-a	IIS6-IIIS1
	D 1300 N[1]	g-a	IIIS1
L 1363 F[1]	L 1363 F[1]	g-c	IIIS2-IIIS3
K 1455 R[4]		a-g	IIIS5-S6
	I1519V[4]	a-g	IIIS5-S6
I 1661 V[1]	I 1661 V[1]	a-g	IVS1-IVS2
I 1670 M[1]	I 1670 M[1]	a-g	IVS2
I 1679 V[2]	I 1679 V[2]	a-g	IVS3
I 1691 V[1]	I 1691 V[1]	a-g	IVS3
	H 1772 Y[4]	c-t	IVS5-S6
N 1822 S[2]	N 1822 S[2]	a-g	IVS5-IVS6

Note: **1.** Amino acid changes that correspond to previously recognized RNA editing sites of variants 13, 18, and 55. **2.** Amino acid changes that correspond to possible RNA editing sites of variants 13, 18, and 55. **3.** Unique editing sites. **4.** Unique editing sites that are situated on the extracellular portion of the pore and that may interact with the binding of Lqh*α*IT.

DISCUSSION:

Functional versus non-functional Para variants in oocytes

In this study, we co-expressed the sixty-four cDNA clones of *para* with TipE to achieve robust expression of sodium currents as previously demonstrated by Warmke et al. (1997). Half of the total variants, thirty-two, had sodium currents large enough for functional analysis (1-2 μA). An additional six variants were functional, however, did not produce sufficient sodium currents for functional analysis (<1 μA). The remaining twenty-six variants did not generate any detectable sodium current (0 μA).

Recently, four TipE-homologous genes (TEH1-4) were identified from D. melanogaster (Derst et al., 2006). The co-expression of three of these genes

(THE 1-3) with *para* (the *para* construct was obtained from Dr. J.C. Cohen; refer to Warmke et al., 1997) in *Xenopus* oocytes also elevated sodium current expression. It would be of interest to determine whether TEH1-4 can boost the low level expression of the six variants in our study. RT-PCR analysis indicated that the expression patterns of TEH1 and TEH4 are under tissue-specific regulation (Derst et al., 2006). Distinct tissue distribution patterns have also been observed for alternative splicing and RNA editing of $BgNa_v$ variants (Tan et al., 2002; Song et al., 2002). The possible tissue-specific co-expression of para variants with TipE or THE1-4 *in vivo* remains to be investigated.

The presence of exon b in *para* and the ortholog B in $BgNa_v$ hampers the expression of $BgNa_V$ and Para channels expressed in oocytes (Song et al., 2004; Song, Personal Communication). Interestingly, four of the six variants with low levels of sodium current expression contain exon B/b, suggesting that this exon could be the cause of poor expression. However, the majority of our functional variants also contain this exon (eighteen out of thirty-two), suggesting that the expression of sodium current is not solely regulated by exon B/b.

At present, we do not know why the twenty-six variants are not functional in *Xenopus* oocytes. Sequencing of the twenty-six nonfunctional variants will reveal whether these variants contain stop codons in the open reading frame thereby generating non-functional channels. It is also possible that these variants require one of the other auxillary subunits, such as TEH1-4, to facilitate expression, or that unidentified sequence features in these variants down-regulate sodium current expression.

Identification of twenty-nine Para splice types

Theoretically 20,160 splicing types could be formed out of the seven optional exons and four mutually exclusive exons. Interestingly though, we only isolated twenty-nine splice types. Although we may have failed to isolate some low frequency splicing types, we believe these twenty-nine represent the majority of transcripts *in vivo*. A previous study investigating exon use of $BgNa_v$ variants identified 20 splice types from a total of 69 variants (Song et al., 2004). These results suggest that alternative exon usage is regulated, and not formed by random combinations.

Since molecular analysis of a large pool of insect SC full-length cDNA clones has been conducted in both *para* (this study) and $BgNa_v$ (Song et al., 2004), a direct comparison of splice types can be made between the two. The most abundant splice type of *para* (twenty percent) is a, b, d, i, j, k, and l, while the most abundant splice type (fifty-five percent) of $BgNa_v$ is a, f, j, k and l. Intriguingly, the most abundant *para* splice type was not isolated at all from $BgNa_V$ variants (Song et al., 2004). This discrepancy is due in part to the differences in the frequency of exon usage of several alternative exons (described above).

Frequency of alternative splicing of insect sodium channels

Previous studies show that alternative splicing sites of SC genes are extremely conserved among *D. melanogaster, D. virilis, M. domestica,* and *B. germanica* (See Chapter 1). However, the frequencies of alternative exon use are less conserved (Table 5). In general, similar exon frequencies can be observed for closely related species, *D. melanogaster* and *D. virilis,* and even for

M. domestica SCs. The frequency of exon use between *B. germanica, D. melanogaster, D, virilis* and *M. domestica* SCs, however, are more divergent. For example, exon a is frequently used in *D. melangoaster, D. virilis, M. domestica* and *B. germanica* SC variants while exon e is not. Exons b, d, and i are expressed in greater than sixty percent of the *para* (both *D. melanogaster and D. virilis*) and *M. domestica* variants. However, exons b and i are not commonly used in $BgNa_V$ transcripts and use of exon d has not yet been identified in $BgNa_V$. Exons c and f are not frequently used in *D. melangoaster, D. virilis,* or *M. domestica* SC transcripts, but are present in over ninety-eight percent of $BgNa_V$ transcripts. Exon h is used in low frequencies in *para,* both of *D. melanogaster* and *D. virilis,* and in $BgNa_V$, however, this exon is present in all transcripts of Vssc1. The frequency of expression of mutually exclusive exon j is high for *para* and $BgNa_V$ transcripts (eighty-nine and seventy nine percent respectively) but low for Vssc1 (*D. virilis* has not been analyzed for the frequency of exon j)

Identification of Three Novel RNA Editing Sites

Prior to this study, ten A-to-I editing sites were identified in *para* (Palladino et al., 2000), and two were reported in $BgNa_V$ variants (Liu et al., 2004; Song et al., 2004). Five of the ten A-to-I editing sites identified in *para* were also identified in the three sequenced variants (13, 18, and 50). Additionally, we identified three novel A-to-I editing events, resulting in three amino acid changes, two I-to-V and one I-to-M change. Potentially there are more RNA editing sites in these three sequenced variants, however, alternative splicing or a mistake made during PCR can not be ruled out. Investigations into the additional changes

observed revealed three possible U-to-C editing. In a previous study three U-to-C editing sites were reported in $BgNa_V$ variants (Liu et al., 2004; Song et al., 2004). Additionally, there are nine possible A-to-I editing sites and two novel changes that do not conform to either A-to-I or U-to-C editing.

Table 5. Frequencies of Exon Usage in Para, VSSC1, $BgNa_V$

Exon	Para[1]	Para[2]	*D. virilis*[3]	VSSC1[4]	$BgNa_V$[5]
A	71.9	57.3	54.4	91-98	98.5
B	60.9	~80	~70	100	17.4
C	29.7	<30	~20	~0	100
D	70.3	>70	~80	~100	0
E	18.8	~25	~25	<10	17.2
F	9.4	6.7	~10	~10	98.5
H	3.1		21	100	0
I	85.9	~85	81	100	5.8
J	89.1			<25	79.7
K	3.1			78-100	5.8
L	96.9			<25	92.7

1. This study
2. O'Dowd et al., 1995; Thackeray and Ganetzky 1994,
3. Thackeray and Ganetzky, 1995
4. Lee et al., 2002;.
5. Song et al., 2004

Estimates are indicated by '~' marks, '>' means greater-than, and '<' means less than.

It is worthwhile mentioning here that a previously identified U-to-C editing event in both *para* and $BgNa_V$ was not detected in any of these sixty-four variants. This U-to-C editing event results in persistent current (Liu et al., 2004) and none of our thirty-two functional variants exhibited persistent currents. Obviously we have missed this variant in our cloning due to the low frequency of this editing event. For the same reason, we may have missed the isolation of other variants which have low editing frequency and play critical roles in regulating inactivation kinetics *in vivo*.

Identification of High-Voltage Activated and Low-Voltage Activated Para Variants

The functional analysis of our sixty-four *para* cDNA clones revealed a broad spectrum in the voltage-dependences of activation among the variants. In an earlier study performed on $BgNa_V$ variants a broad range in the voltage-dependency of activation was also identified (Song et al., 2004). The range of the voltage-dependences of activation for the $BgNa_V$ variants was from -24.9 mV to -43.9 mV (Song et al., 2004). In this study we, for the first time, identified several LVA and HVA sodium channels. Variant 18 is an LVA channel with a voltage-dependence of activation of -46 mV. Variants 50 and 55 are extreme HVA channels with voltage dependences less than -10 mV. An additional sixteen of our variants activate at potentials less than that previously reported for $BgNa_V$ variants (less than -24.9 mV). The molecular basis of the LVA and HVA gating characteristics remained to be identified.

Mammalian SCs exhibit distinct voltage dependences of activation (Chapter 1 – Table 1). In general, those isoforms, that are predominantly located in the central nervous system (CNS; Na_V 1.1, 2, 3, and 6) activate at more depolarized (i.e., positive) potentials than those predominantly located in the peripheral nervous system (PNS; Na_V 1.7, 8, and 9). The cardiac sodium channel, Na_V 1.5, and isoform Na_V 1.9 activate at more hyperpolarized (i.e., negative) potentials than the remaining mammalian sodium channels (Chapter 1 - Table 2). The half-maximal voltages for activation of $Na_V1.5$ (heart SC) are -45 or -46 mV and $Na_V1.9$ (DRG neurons) are -47 or -54 mV, similar to that of the Para variant 18.

The terms, HVA and LVA, are well-established to describe distinct calcium channel families (review by Yunker, 2003). LVA calcium channels, such as $Ca_V3.1$, 2, and 3, activate at hyperpolarized potentials near resting membrane potential, while HVA calcium channels, such as $Ca_V1.1$, 2, 3, and 4, require strong depolarization above resting membrane potential in order to activate the channel (review by Catterall et al., 2005). LVA calcium channels are responsible for the repetitive firing of action potentials in pacemaker cells while HVA channels are involved in excitation-contraction coupling, hormone release, and neurotransmitter release (review by Catterall et al., 2005).

Whether these Para LVA channels play a similar role and have similar tissue distributions as mammalian Na_V 1.5 and LVA calcium channels remains to be determined. Both $Na_V1.5$ and LVA calcium channels are localized in the heart muscle and both facilitate spontaneous firing. While we do not know the tissue distribution pattern of variant 18, it may be expressed in tissues and cells with pace-making activities. Studies of cockroach terminal abdominal ganglia DUM neurons characterized pacemaking activities as the result of LVA sodium channels (Lapied et al., 1998). These LVA sodium channels activated at potentials of -50 mV, which corresponds to the resting membrane potential of DUM neurons in cockroach terminal abdominal ganglia. It was hypothesized in this study that background channels are essential in the instigation and continuation of spontaneous firing because activation of these channels depolarize membrane potentials which in turn activate additional channels and result in action potential propagation. It would be of interest to determine the

tissue distribution of variant 18, and determine if this variant is responsible for the pace-making activities observed in the DUM neurons.

Identification of an Lqhαit-resistant Para variant

The specific amino acids of the SV that are critical for Lqhαit binding remain elusive. Identification of an Lqhαit-resistant variant, #21, from our survey of Lqhαit sensitivity of sixty-four Para variants provided valuable information for further elucidating the molecular determinants of the Lqhαit binding site on the sodium channel.

Photoaffinity labeling, site-directed mutagenesis studies, and site-directed antibodies against individual extracellular loops revealed DIS5-S6, DIVS5-S6, and DIVS3-S4 are involved in α-scorpion toxin binding on mammalian sodium channels (references in Rogers et al., 1996). We found a single novel amino acid change in variant 8 that is located in the extracellular loop connecting DIIIS5 to DIIIS6 that may confer the observed sensitivity of this variant to Lqhαit binding (K1455R). The insensitive variant 21 has two novel amino acid changes (I1519V and Y1772H) that are located in the extracellular loops connecting S5 to S6 of DIII and DIV that may interact with Lqhαit and inhibit binding of the toxin to the channel resulting in a resistant variant. Future mutagenesis studies are needed in order to verify the involvement of these amino acids in Lqhαit binding.

LITERATURE SITED

Agnew WS, Moore AC, Levinson SR, Raftery MA. 1980. Identification of a large molecular weight peptide associated with a tetrodotoxin binding protein from the electroplax of Electrophorus electricus. *Biochem Biophys Res Commun* 92:860-6

Beneski DA, Catterall WA. 1980. Covalent labeling of protein components of the sodium channel with a photoactivable derivative of scorpion toxin. *Proc Natl Acad Sci U S A* 77:639-43

Castella C, Amichot M, Berge JB, Pauron D. 2001. DSC1 channels are expressed in both the central and the peripheral nervous system of adult Drosophila melanogaster. *Invert Neurosci* 4:85-94

Catterall WA. 1986. Molecular properties of voltage-sensitive sodium channels. *Annu Rev Biochem* 55:953-85

Catterall WA. 2000. From ionic currents to molecular mechanisms: the structure and function of voltage-gated sodium channels. *Neuron* 26:13-25

Catterall WA, Goldin AL, Waxman SG. 2003. International Union of Pharmacology. XXXIX. Compendium of voltage-gated ion channels: sodium channels. *Pharmacol Rev* 55:575-8

Catterall WA, Goldin AL, Waxman SG. 2005. International Union of Pharmacology. XLVII. Nomenclature and structure-function relationships of voltage-gated sodium channels. *Pharmacol Rev* 57:397-409

Cestele S, Catterall WA. 2000. Molecular mechanisms of neurotoxin action on voltage-gated sodium channels. *Biochimie* 82:883-92

Chen H, Gordon D, Heinemann SH. 2000. Modulation of cloned skeletal muscle sodium channels by the scorpion toxins Lqh II, Lqh III, and Lqh alphaIT. *Pflugers Arch* 439:423-32

Claes L, Del-Favero J, Ceulemans B, Lagae L, Van Broeckhoven C, De Jonghe P. 2001. De novo mutations in the sodium-channel gene SCN1A cause severe myoclonic epilepsy of infancy. *Am J Hum Genet* 68:1327-32

Derst C, Walther C, Veh RW, Wicher D, Heinemann SH. 2006. Four novel sequences in Drosophila melanogaster homologous to the auxiliary Para sodium channel. *Biochem Biophys Res Commun* 339:938-48

Dong K. 1997. A single amino acid change in the para sodium channel protein is associated with knockdown-resistance (kdr) to pyrethroid insecticides in German cockroach. *Insect Biochem Mol Biol* 27:93-100

Eaholtz G, Colvin A, Leonard D, Taylor C, Catterall WA. 1999. Block of brain sodium channels by peptide mimetics of the isoleucine, phenylalanine, and methionine (IFM) motif from the inactivation gate. *J Gen Physiol* 113:279-94

Eaholtz G, Scheuer T, Catterall WA. 1994. Restoration of inactivation and block of open sodium channels by an inactivation gate peptide. *Neuron* 12:1041-8

Germeraad S, O'Dowd D, Aldrich RW. 1992. Functional assay of a putative Drosophila sodium channel gene in homozygous deficiency neurons. *J Neurogenet* 8:1-16

Goldin AL. 1999. Diversity of mammalian voltage-gated sodium channels. *Ann N Y Acad Sci* 868:38-50

Goldin AL, Barchi RL, Caldwell JH, Hofmann F, Howe JR, et al. 2000. Nomenclature of voltage-gated sodium channels. *Neuron* 28:365-8

Goldin AL. 2002. Evolution of voltage-gated Na^+ channels. *J Exp Biol* 205:575-84

Goldin AL. 2003. Mechanisms of sodium channel inactivation. *Curr Opin Neurobiol* 13:284-90

Gordon D, Martin-Eauclair MF. 1996. Scorpion toxins affecting sodium current inactivation bind to distinct homologous receptor sites on rat brain and insect sodium channelsd. *J Biol Chem* 271:8034-45

Guy HR, Seetharamulu P. 1986. Molecular model of the action potential sodium channel. *Proc Natl Acad Sci U S A* 83:508-12

Heinemann SH, Terlau H, Stuhmer W, Imoto K, Numa S. 1992. Calcium channel characteristics conferred on the sodium channelby single mutations. *Nature* 356:441-3

Hille B. 1984. *Ionic Channels of Excitable membranes* Sinauer Associates, Inc, Sunderland, MA

Hodgkin AL, Huxley AF. 1952a. The dual effect of membrane potential on sodium conductance in the giant axon of Loligo. *J Physiol* 116:497-506

Hodgkin AL, Huxley AF. 1952b. A quantitative description of membrane current and its application to conduction and excitation in nerve. *J Physiol* 117:500-44

Hong CS, Ganetzky B. 1994. Spatial and temporal expression patterns of two sodium channel genes in Drosophila. *J Neurosci* 14:5160-9

Isom LL. 2001. Sodium channel beta subunits: anything but auxiliary. *Neuroscientist* 7:42-54

Kelly P, Yang WS, Costigan D, Farrell MA, Murphy S, Hardiman O. 1997. Paramyotonia congenita and hyperkalemic periodic paralysis associated with a Met 1592 Val substitution in the skeletal muscle sodium channel alpha subunit--a large kindred with a novel phenotype. *Neuromuscul Disord* 7:105-11

Kontis KJ, Rounaghi A, Goldin AL. 1997. Sodium channel activation gating is affected by substitutions of voltage sensor positive charges in all four domains. *J Gen Physiol* 110:391-401

Kontis KJ, Goldin AL. 1993. Site-directed mutagenesis of the putative pore region of the rat IIA sodium channel. *Mol Pharmacol.* 43:635-44

Lee SH, Ingles PJ, Knipple DC, Soderlund DM. 2002. Developmental regulation of alternative exon usage in the house fly Vssc1 sodium channel gene. *Invert Neurosci* 4:125-33

Lee D, Gurevitz M, Adams ME. 2000. Modification of Synaptic Transmission and Sodium Channel Inactivation by the Insect-Selective Scorpion Toxin Lqh*α*IT. *J. Neurophysiol* 83:1181-7

Liu Z, Chung I, Dong K. 2001. Alternative splicing of the BSC1 gene generates tissue-specific isoforms in the German cockroach. *Insect Biochem Mol Biol* 31:703-13

Liu Z, Song W, Dong K. 2004. Persistent tetrodotoxin-sensitive sodium current resulting from U-to-C RNA editing of an insect sodium channel. *Proc Natl Acad Sci U S A* 101:11862-7

Loughney K, Kreber R, Ganetzky B. 1989. Molecular analysis of the para locus, a sodium channel gene in Drosophila. *Cell* 58:1143-54

McPhee JC, Ragsdale DS, Scheuer T, Catterall WA. 1998. A critical role for the S4-S5 intracellular loop in domain IV of the sodium channel alpha-subunit in fast inactivation. *J Biol Chem* 273:1121-9

Noda M, Ikeda T, Suzuki H, Takeshima H, Takahashi T, et al. 1986. Expression of functional sodium channels from cloned cDNA. *Nature* 322:826-8

Noda M, Shimizu S, Tanabe T, Takai T, Kayano T, et al. 1984. Primary structure of Electrophorus electricus sodium channel deduced from cDNA sequence. *Nature* 312:121-7

O'Dowd DK, Aldrich RW. 1988. Voltage-clamp analysis of sodium channels in wild-type and mutant Drosophila neurons. *J Neurosci* 8:3633-43

O'Dowd DK, Germeraad SE, Aldrich RW. 1989. Alterations in the expression and gating of Drosophila sodium channels by mutations of the para gene *Neuron*. 4:1301-11

O'Dowd DK, Gee JR, Smith MA. 1995. Sodium current density correlates with expression of specific alternatively spliced sodium channel mRNAs in single neurons. *J Neurosci* 15:4005-12

Palladino MJ, Keegan LP, O'Connell MA, Reenan RA. 2000a. dADAR, a Drosophila double-stranded RNA-specific adenosine deaminase is highly developmentally regulated and is itself a target for RNA editing. *Rna* 6:1004-18

Palladino MJ, Keegan LP, O'Connell MA, Reenan RA. 2000b. A-to-I pre-mRNA editing in Drosophila is primarily involved in adult nervous system function and integrity. *Cell* 102:437-49

Patton DE, West JW, Catterall WA, Goldin AL. 1992. Amino acid residues required for fast Na(+)-channel inactivation: charge neutralizations and deletions in the III-IV linker. *Proc Natl Acad Sci U S A* 89:10905-9

Ramaswami M, Tanouye MA. 1989. Two sodium-channel genes in Drosophila: implications for channel diversity. *Proc Natl Acad Sci U S A* 86:2079-82

Rogers JC, Qu Y, Tanada TN, Scheuer T, Catterall WA. Molecular determinants of high affinity binding of alpha-scorpion toxin and sea anemone toxin in the S3-S4 extracellular loop in domain IV of the Na+ channel alpha subunit. *J Biol Chem* 271:15950-62

Rohl CA, Boeckman FA, Baker C, Scheuer T, Catterall WA, Klevit RE. 1999. Solution structure of the sodium channel inactivation gate. *Biochemistry* 38:855-61

Saito M, Wu CF. 1991. Expression of ion channels and mutational effects in giant Drosophila neurons differentiated from cell division-arrested embryonic neuroblast. *J. Neurosci* 7:2135-50

Salkoff L, Butler A, Wei A, Scavarda N, Giffen K, et al. 1987. Genomic organization and deduced amino acid sequence of a putative sodium channel gene in Drosophila. *Science* 237:744-9

Siddiqi O, Benzer S. 1976. Neurophysiological defects in temperature-sensitive paralytic mutants of Drosophila melanogaster. *Proc Natl Acad Sci U S A* 73:3253-7

Silver K, Soderlund DM. 2005. State-dependent block of rat Nav1.4 sodium channels expressed in xenopus oocytes by pyrazoline-type insecticides. *Neurotoxicology* 26:397-406

Soderlund DM. 2005. Sodium channels. *Comp Mol Insect Sci* 5:1-24

Song W, Liu Z, Tan J, Nomura Y, Dong K. 2004. RNA editing generates tissue-specific sodium channels with distinct gating properties. *J Biol Chem* 279:32554-61

Song W, Liu Z, Dong K. 2006. Molecular basis of differential senstivity of insect sodium channels to DCJW, a bioactive metabolite of the oxadiazine insecticide indoxacarb. *Neurotoxicology* 2:237-44

Striessnig J, Glossmann H, Catterall WA. 1990. Identification of a phenylalkylamine binding region within the alpha 1 subunit of skeletal muscle Ca2+ channels. *Proc Natl Acad Sci U S A* 87:9108-12

Stuhmer W, Conti F, Suzuki H, Wang XD, Noda M, et al. 1989. Structural parts involved in activation and inactivation of the sodium channel. *Nature* 339:597-603

Suzuki DT, Grigliatti T, Williamson R. 1971. Temperature-sensitive mutations in Drosophila melanogaster. VII. A mutation (para-ts) causing reversible adult paralysis. *Proc Natl Acad Sci U S A* 68:890-3

Tan J, Liu Z, Nomura Y, Goldin AL, Dong K. 2002a. Alternative splicing of an insect sodium channel gene generates pharmacologically distinct sodium channels. *J Neurosci* 22:5300-9

Tan J, Liu Z, Tsai TD, Valles SM, Goldin AL, Dong K. 2002b. Novel sodium channel gene mutations in Blattella germanica reduce the sensitivity of expressed channels to deltamethrin. *Insect Biochem Mol Biol* 32:445-54

Terlau H, Heinemann SH, Stuhmer W, Pusch M, Conti F, et al. 1991. Mapping the site of block by tetrodotoxin and saxitoxin of sodium channel II. *FEBS Lett* 293:93-6

Thackeray JR, Ganetzky B. 1994. Developmentally regulated alternative splicing generates a complex array of Drosophila para sodium channel isoforms. *J Neurosci* 14:2569-78

Thackeray JR, Ganetzky B. 1995. Conserved alternative splicing patterns and splicing signals in the Drosophila sodium channel gene para. *Genetics* 141:203-14

Ulbricht W. 2005. Sodium channel inactivation: molecular determinants and modulation. *Physiol Rev* 85:1271-301

Vais H, Williamson MS, Devonshire AL, Usherwood PN. 2001. The molecular interactions of pyrethroid insecticides with insect and mammalian sodium channels. *Pest Manag Sci* 57:877-88

Vassilev P, Scheuer T, Catterall WA. 1989. Inhibition of inactivation of single sodium channels by a site-directed antibody. *Proc Natl Acad Sci U S A* 86:8147-51

Vassilev PM, Scheuer T, Catterall WA. 1988. Identification of an intracellular peptide segment involved in sodium channel inactivation. *Science* 241:1658-61

Wang SY, Wang GK. 2003. Voltage-gated sodium channels as primary targets of diverse lipid-soluble neurotoxins. *Cell Signal* 15:151-9

Warmke JW, Reenan RA, Wang P, Qian S, Arena JP, et al. 1997. Functional expression of Drosophila para sodium channels. Modulation by the membrane protein TipE and toxin pharmacology. *J Gen Physiol* 110:119-33

West JW, Patton DE, Scheuer T, Wang Y, Goldin AL, Catterall WA. 1992. A cluster of hydrophobic amino acid residues required for fast Na(+)-channel inactivation. *Proc Natl Acad Sci U S A* 89:10910-4

Wu CF, Ganetzky B. 1980. Genetic alteration of nerve membrane excitability in temperature-sensitive paralytic mutants of Drosophila melanogaster. *Nature* 286:814-6

Yu FH, Westenbroek RE, Silos-Santiago I, McCormick KA, Lawson D, et al. 2003. Sodium channel beta4, a new disulfide-linked auxiliary subunit with similarity to beta2. *J Neurosci* 23:7577-85

Zhao Y, Yarov-Yarovoy V, Scheuer T, Catterall WA. 2004. A gating hinge in Na+ channels; a molecular switch for electrical signaling. *Neuron* 41:859-65

Zhou W, Chung I, Liu Z, Goldin AL, Dong K. 2004. A voltage-gated calcium-selective channel encoded by a sodium channel-like gene. *Neuron* 42:101-112